

Cite this: *Chem. Sci.*, 2020, **11**, 4954

All publication charges for this article have been paid for by the Royal Society of Chemistry

Received 10th February 2020
Accepted 20th April 2020DOI: 10.1039/d0sc00819b
rsc.li/chemical-science

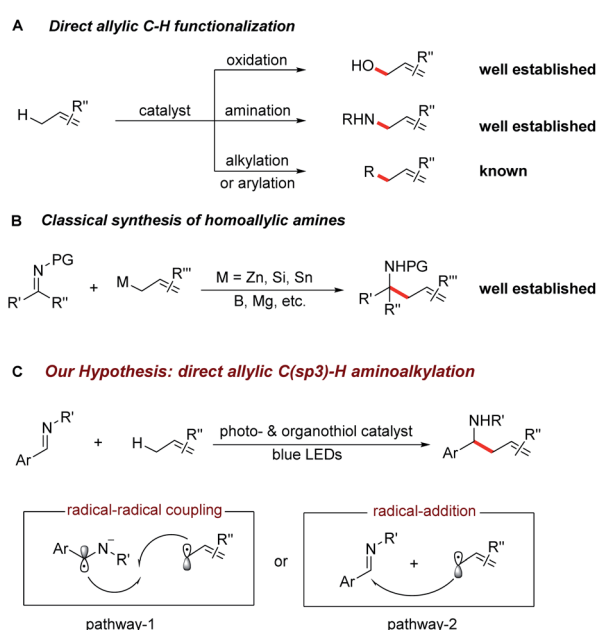
1. Introduction

The selective C–H bond functionalization has expanded rapidly over the past decade owing to its tremendous potential to streamline the synthesis of natural products, pharmaceuticals, agrochemicals and materials.^{1,2} Allylic C–H activations are of particular interest due to the synthetic versatility of the resulting alkenes and opportunities for further functionalization. Despite the recent progress in the direct oxidation,³ amination,⁴ carboxylation,⁵ alkylation⁶ and arylation⁷ of allylic C–H bonds, direct C(sp³)–C(sp³) bond formations remain a major challenge for synthetic organic chemistry.

Homoallylic amines are versatile building blocks and precursors for the synthesis of bioactive molecules and functional materials.^{8a} Thus, routes for their efficient preparation have received considerable interest (Scheme 1A and B).⁸ Although advances in conventional organic synthesis have been achieved, several issues need to be addressed. These include the frequent requirement of cryogenic conditions, multi-step syntheses of the organometallic reagents and the generation of stoichiometric amounts of by-products.⁹ Recent developments in visible light photocatalyzed reactions have enabled new synthetic pathways towards the functionalization of imines.^{10,11} Notably, the polarity-reversed allylation of imines with prefunctionalized alkenes has been reported.^{10e} This reaction, however, requires stoichiometric amount of Hantzsch ester as electron/proton donor and activator. We recently questioned whether the direct coupling between an aminoalkyl

moiety and an allylic C(sp³)–H bond of simple olefins could be feasible. This strategy is generically useful considering it can overcome the challenges of functional group compatibility associated with preparation of allylation precursors and the use of excess reductants. Therefore, it could offer a wealth of opportunities for elaboration of both complex molecules and feedstock olefins.

In line with our recent reports on reductive Umpolung of imines^{10f,g} as well as recent development on synergistic organo- and photoredox catalysis,¹² we envisioned that upon visible



^aInstitute of Organic Chemistry, RWTH Aachen University, Landoltweg 1, D-52074 Aachen, Germany. E-mail: magnus.rueping@rwth-aachen.de; long.huang@rwth-aachen.de

^bKAUST Catalysis Center, KCC, King Abdullah University of Science and Technology, KAUST, Thuwal, 23955-6900, Saudi Arabia

† Electronic supplementary information (ESI) available. See DOI: 10.1039/d0sc00819b

Scheme 1 (A) The reaction development of direct allylic C–H activation of olefins. (B) Classical methods towards homoallylic amines synthesis. (C) Photoredox activation of allylic C(sp³)–H bonds for the homoallylic amines synthesis, initial proposed reaction pathways.



light irradiation, the resulting oxidizing excited state of a photocatalyst $\text{PC}^{(n-1)+}$ * could be quenched by a thiol catalyst RSH through proton coupled electron transfer (PCET)¹³ in the presence of a basic additive¹⁴ to give the corresponding reduced $\text{PC}^{(n-1)+}$ complex and a transient thiyl radical $\text{RS}\cdot$.¹⁵ The generated electrophilic thiyl radical would then react with the alkene substrate (allylic C–H bond dissociation energy BDE is about 340 kJ mol^{−1}) *via* hydrogen atom transfer to form an allylic radical along with the regeneration of thiol catalyst ($\text{S}-\text{H}$ BDE is typically 365 kJ mol^{−1}).¹⁶

Next, the oxidation of $\text{PC}^{(n-1)+}$ species with imine $\text{ArCH}=\text{NR}'$ *via* single electron transfer would result in the formation of the aminoalkyl radical anion¹⁷ and the following radical–radical cross coupling¹⁸ with the allylic radical¹⁹ would result in the desired C–C bond formation (pathway 1). Alternatively, the allylic radical could add to the imine to form a N-centred radical, which is subsequently reduced by $\text{PC}^{(n-1)+}$ to give the desired product (pathway 2). Herein, we report the successful development of a new protocol for the direct alkylation of allylic $\text{C}(\text{sp}^3)-\text{H}$ bonds *via* synergistic organo- and photoredox catalysis (Scheme 1C) and provide insight into the reaction mechanism of this efficient addition reaction.

2. Results and discussions

Based on our mechanistic hypothesis, we first evaluated the reaction conditions with imine **1a** and cyclohexene **2a**. To our delight, we found that the reaction of **1a** with **2a** (5 equiv) in the presence of $[\text{Ir}(\text{ppy})_2(\text{dtbbpy})]\text{PF}_6$ **3a** (ppy = 2,2'-bipyridine, d'tbbpy = 4,4'-di-*tert*-butyl-2,2'-bipyridine, $E_{1/2}^{\text{III/II}} = +0.66$ V *vs.* SCE in MeCN)²⁰ (1 mol%), organocatalyst **4** (5 mol%) and Li_2CO_3 (20 mol%) in DMF under irradiation with 24 W blue LEDs ($\lambda_{\text{max}} = 405$ nm) afforded the desired homoallylic amine product **5a** in 81% yield (Table 1, entry 1). Remarkably, we did not observe any reductive homocoupling product under these reaction conditions.^{10g} Control experiments confirmed that the reaction did not proceed in the absence of the photocatalyst and light (entries 2 and 3). Moreover, only traces of the desired product were obtained in the absence of thiol **4**, indicating the necessity of the hydrogen atom transfer (HAT) catalyst (entry 4). The use of other Ir-based photocatalysts gave **5a** in lower yields (entries 5–7). In sharp contrast, only 5% of the desired coupling product was obtained when less reducing $\text{Ru}(\text{bpy})_3(\text{PF}_6)_2$ ($E_{1/2}^{\text{II/I}} = -1.35$ V *vs.* SCE)²¹ was employed as photocatalyst (entry 8). The organic photocatalyst mesityl acridinium which is known as a weak reductant in its reduced form was next examined,²² but no product was observed (entry 9). Interestingly, a moderate yield was obtained in the absence of a basic additive (entry 10). In addition, we found that DMF was a suitable solvent while MeCN was inferior (entry 11). Notably, 34% of **5a** was obtained when **2a** was used as limiting reagent (entry 12). The use of other thiols failed to improve the yield (see ESI†).

Under the optimized reaction conditions, we next screened various imines **1** in reaction with cyclohexene **2a**. As shown in Table 2, a wide range of *N*-aryl imines with various substituents on the aryl ring underwent the aminoalkylation smoothly, affording the desired homoallylic amines **5b–k** in good to

Table 1 Optimization of the reaction conditions^a

1	None
2	No photocatalyst
3	No light
4	No thiol 4
5	Photocatalyst 3b instead of 3a
6	Photocatalyst 3c instead of 3a
7	Photocatalyst 3d instead of 3a
8	Photocatalyst 3e instead of 3a
9	Photocatalyst 3f instead of 3a
10	No Li_2CO_3
11	MeCN as solvent
12	2a as limiting reagent

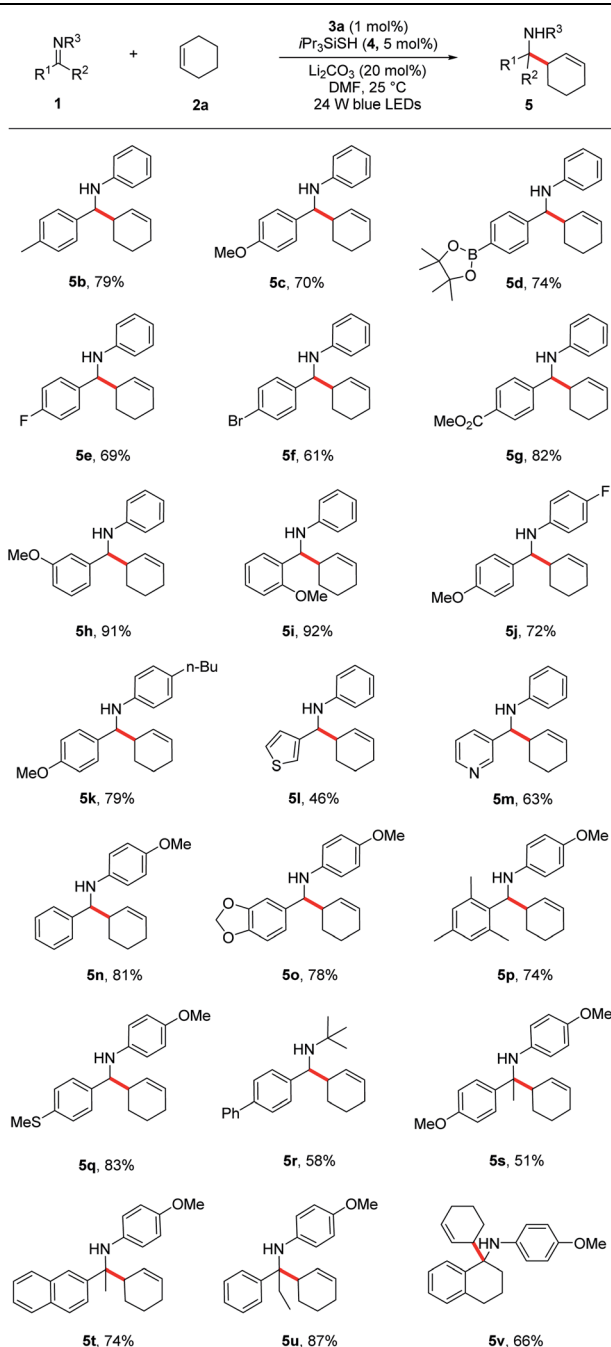
^a Reaction conditions: **1a** (0.2 mmol), cyclohexene **2a** (1.0 mmol), Li_2CO_3 (20 mol%), $i\text{Pr}_3\text{SiSH}$ **4** (5 mol%), **3a–f** (1 mol%), rt, solvent (2 mL), 24 W LEDs (450 nm), 24 h. ^b Yield of product after isolation.

excellent yields (61–92%) regardless of their electronic nature as well as substituent position. Notably, imines containing heterocyclic groups such as thiophene and pyridine were compatible with the reaction conditions and gave the corresponding products **5l** and **5m** in 46% and 63% yield, respectively. Moreover, the reaction proceeded in excellent yields for imines bearing the readily removable *N*-*p*-methoxyphenyl group (**5n–q**, 74–83%). In addition to *N*-aryl imines, imine **1r** derived from an alkyl amine was also tolerated, albeit in moderate yield (**5r**, 58%).

Encouraged by these results, we next evaluated more challenging ketimine substrates for the construction of all-carbon quaternary centers. Not surprisingly, aromatic ketimines were converted to the corresponding homoallylamines in good yields (**5s–v**, 51–87%). Next, we evaluated the scope of allylic radicals that can be generated with this protocol. Under the optimized conditions, a variety of cyclic and acyclic alkenes were successfully aminoalkylated using imine **1a**, furnishing the corresponding products in good yields (Table 3). In addition to cyclohexene **2a** described above, several other cyclic alkenes **2b–d** (five, seven and eight membered derivatives) were tested and the corresponding homoallylic amines **6a–d** were prepared in good to excellent yields under the reaction conditions (**6a–d**, 62–



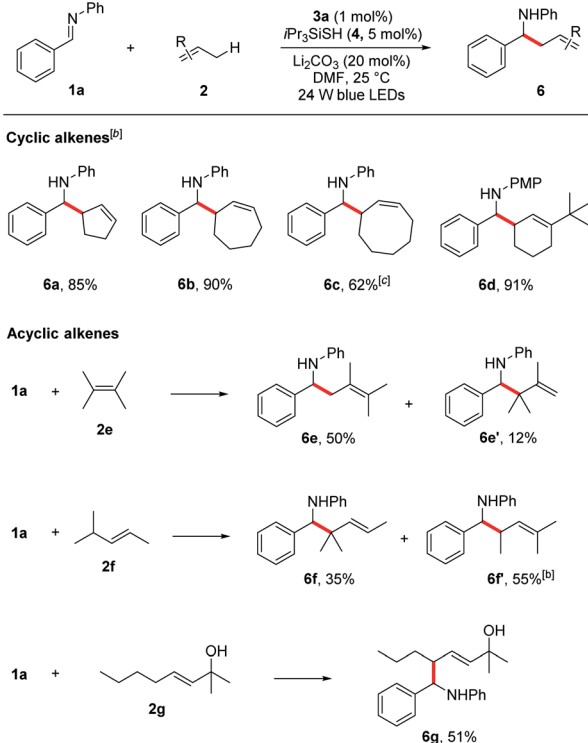
Table 2 Scope of various imine substrates^a



^a Reaction conditions: imine **1** (0.3 mmol), cyclohexene **2a** (1.5 mmol), Li₂CO₃ (20 mol%), *i*Pr₃SiSH **4** (5 mol%), **3a** (1 mol%), DMF (1.5 mL), 24 W LEDs (450 nm), rt, 24 h; yields after isolation; dr between 1 : 1 to 1.2 : 1.

90%). An excellent regioselectivity was observed with 1-(*tert*-butyl)cyclohex-1-ene (**2d**), indicating that steric effects play a predominant role in determining the regioselectivity. For asymmetrically substituted alkene **2f** which has two different C–H bonds at the allylic sites, isomers of aminoalkylation were observed. The selective formation of **6f** and **6f'** suggests that the proton abstraction of allylic methine C–H bonds is favoured

Table 3 Scope of alkene substrates^{ab}



^a Reaction conditions: imine **1a** (0.2 mmol), alkene **2** (1.0 mmol), Li₂CO₃ (20 mol%), iPr₃SiH **4** (5 mol%), **3a** (1 mol%), DMF (1.0 mL), 24 W LEDs (450 nm), rt, 24 h; yields after purification. ^b dr between 1 : 1 to 1.2 : 1. ^c iPr₃SiH **4** (10 mol%).

over primary C-H bonds due to the formation of more stabilized carbon centred radical. It is notable that unprotected allylic alcohol **2g** was also aminoalkylated providing the corresponding product **6g** in 51% yield.

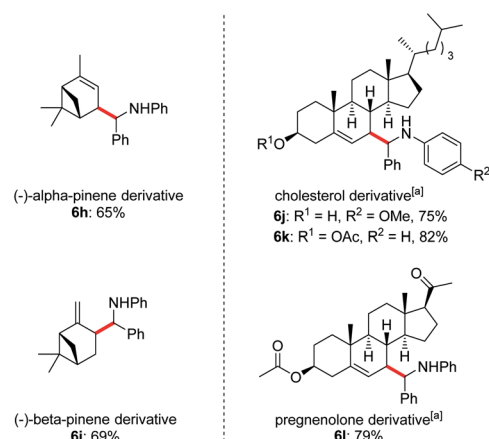


Fig. 1 Late-stage diversification of complex molecules. Reaction conditions: imine **1** (0.2 mmol), alkene **2** (1.0 mmol), Li_2CO_3 (20 mol%), $i\text{Pr}_3\text{SiSH}$ **4** (5 mol%), **3a** (1 mol%), DMF (1.0 mL), 24 W LEDs (450 nm), rt, 24 h, for dr see ESI.[†] **2** (0.6 mmol), $i\text{Pr}_3\text{SiSH}$ **4** (10 mol%), DMF (2 mL). ^b Isomers ratios: **6h** (1.2 : 1 : 1 : 1), **6i** (3 : 3 : 1 : 1), **6j** (1.6 : 1.6 : 1 : 1), **6k** (1.2 : 1 : 1 : 1), **6l** (1.9 : 1.9 : 1).

Owing to the wide applications of natural product modification in the fields of medicine, health science, pharmacy and biology, we subsequently focused on the aminoalkylation of several naturally occurring substrates as well as their derivatives (Fig. 1). Both regioisomers of pinenes could be converted to the homoallylic amines **6h** and **6i** with excellent regioselectivities at the methylene C–H bonds. This can be explained by the electrophilic thiol radical selectively abstracts the allylic C–H bond to form the more stabilized radical of pinenes. Meanwhile, the steric effect also plays a major part in determining the regioselectivity, the C–C bond formation selectively takes place in the sterically less-hindered allylic position. Steroid derivatives such as cholesterol and pregnenolone could also be functionalized

under the photoredox conditions and the aminoalkylation took place selectively at the allylic position, affording the corresponding diastereomers **6j–l** in good yields. In comparison with literature precedent,^{7c} the low to moderate diastereoselectivities indicates that a possible different reaction pathway was involved for the current transformation.

In order to gain some insight into the reaction mechanism, we first performed radical inhibition experiments. The reaction was greatly suppressed in the presence of various radical inhibitors, indicating the involvement of a radical process. It is noteworthy that radical initiators failed to give any product even at elevated temperature (see ESI†). Next, a series of experiments were conducted to better understand the nature of

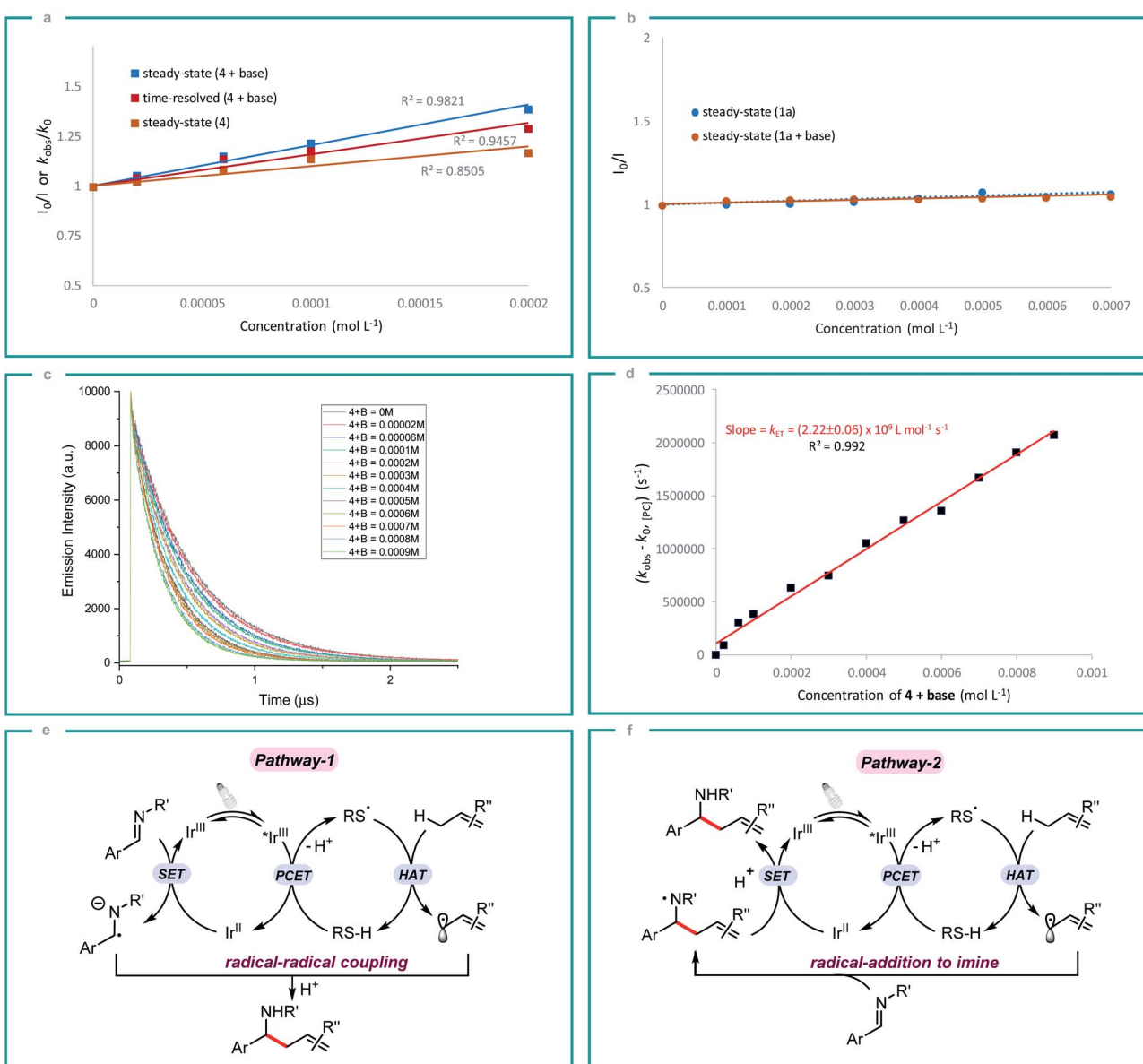


Fig. 2 (a) Steady-state and time-resolved Stern–Volmer quenching of **3a** with **4** and the mixture of **4 + base** (Li_2CO_3); (b) Steady-state Stern–Volmer quenching experiment with **1a** and the mixture of **1a + base** (Li_2CO_3); (c) phosphorescence lifetimes of excited-state photocatalyst ***3a** (1×10^{-5} M) at different concentrations of quencher mixture **4 + base** ($B = \text{Li}_2\text{CO}_3$). (d) Stern–Volmer analysis yielded a rate constant, k_{ET} , of 2.22×10^9 L mol⁻¹ s⁻¹ by the PCET between ***3a** and **4** in the presence of base; (e & f) proposed mechanistic pathways for aminoalkylation of allylic C(sp³)-H bonds.



photoinduced single electron transfer step. The photocatalyst $[\text{Ir}(\text{ppy})_2(\text{dtbbpy})]\text{PF}_6$ **3a** on photoexcitation can result in a long-lived triplet excited state ${}^3\text{a}$ ($\tau_0 = 454.71 \pm 0.30$ ns in DMF, Fig. S1†), which can result in SET in the presence of suitable quencher. Therefore, Stern–Volmer quenching experiments were performed in order to confirm the quenching of **3a**. Initially, steady-state fluorescence quenching of **3a** using different concentrations of silanethiol **4** was carried out in the presence of Li_2CO_3 , where a predominant quenching was observed with a linear correlation (Fig. 2a). Further, a linear correlation similar to steady-state experiments was also observed by time-resolved emission spectroscopy studies where excited-state life-time of ${}^3\text{a}$ is quenched by different concentrations of **4** in the presence of Li_2CO_3 (Fig. 2a). Linear correlation by both the time-resolved and steady-state Stern–Volmer quenching experiments reveal the dynamic quenching of triplet excited-state of ${}^3\text{a}$ by **4** in the presence of base. Next, a similar quenching experiments was carried out in the absence of base which also displayed considerable quenching of ${}^3\text{a}$ (Fig. 2a). In-line with the observed result, a moderate yield of 55% of homoallylic amine **5a** was obtained in the absence of a basic additive (Table 1, entry 10). Simultaneous steady-state Stern–Volmer quenching studies using **1a** proved that there is no quenching of excited-state of ${}^3\text{a}$ even in the absence and presence of base (Fig. 2b). In order to understand the electron transfer event better, the electron transfer rate constant k_{ET} was determined by time-resolved emission spectroscopy measurements. An electron transfer rate constant, $k_{\text{ET}} = (2.22 \pm 0.06) \times 10^9 \text{ L mol}^{-1} \text{ s}^{-1}$ was obtained by plotting the difference between the observed rate constant (k_{obs}) and rate constant without quencher (k_0) versus different concentrations of **4** in presence of base which gave a linear fit (Fig. 2c and d).

Initially, we assumed that the alkylation process may proceed through the radical–radical coupling pathway (Fig. 2e, pathway-1), where the allylic radical couples with the persistent radical anion intermediate that is generated by the SET reduction of imine. However, the lack of informative byproducts formation including reduced amine and vicinal diamine derived from the *N*-centered radical anion prompted us to think otherwise. And if such an intermediate is involved in the reaction process, there should be a yield dependence on the electronics of the imine. Based on our substrate scope both electron rich (**1b**) and electron deficient (**1g**) imines gave the expected product in good yield which indicates the possibility of an alternate pathway. Furthermore, the reduction potential of imines **1a** and **1c** ($E_{1/2} = -1.91$ and -2.01 V vs. SCE respectively)^{10c} is very low compared to the redox potential of photocatalyst **3a** ($\text{Ir}^{\text{III}}/\text{Ir}^{\text{II}} = -1.51$ V) which does not favour the formation of radical anion intermediate. Nevertheless, both the imines **1a** and **1c** gave the expected product in good yield. All these observations strongly indicate that the reaction proceeds through the *N*-centered radical intermediate which is generated by the allylic radical addition to the imine. This *N*-centered radical subsequently gets reduced by Ir^{II} to give the expected product (Fig. 2f, pathway-2).²³

In conclusion, we developed a new method for the efficient synthesis of homoallylic amines through the direct alkylation of

allylic $\text{C}(\text{sp}^3)\text{–H}$ bonds of simple alkenes with imines by using the combination of photoredox and organocatalysis. The reaction tolerates a wide range of functional groups and proceeds under mild reaction conditions. The reactivity and utility of this protocol can be further emphasized in the late stage allylic $\text{C}(\text{sp}^3)\text{–H}$ bond functionalization of a range of complex natural products and derivatives. The strategy developed herein could be of relevance for organic synthesis as well as pharmaceutical development and may inspire the discovery other direct allylic $\text{C}(\text{sp}^3)\text{–H}$ functionalizations.

Conflicts of interest

There are no conflicts to declare.

Acknowledgements

This work was financially supported by the King Abdullah University of Science and Technology (KAUST), Saudi Arabia, Office of Sponsored Research (URF/1/3754).

References

- For selected reviews on C–H functionalization in the synthesis of complex molecules, see: (a) A. F. M. Noisier and M. A. Brimble, *Chem. Rev.*, 2014, **114**, 8775–8806; (b) T. Cernak, K. D. Dykstra, S. Tyagarajan, P. Vachal and S. W. Krska, *Chem. Soc. Rev.*, 2016, **45**, 546–576; (c) P. Tao and Y. Jia, *Sci. China: Chem.*, 2016, **59**, 1109–1125.
- For reviews on photoredox catalysis in C–H functionalizations, see: (a) D. C. Fabry and M. Rueping, *Acc. Chem. Res.*, 2016, **49**, 1969–1979; (b) X.-Q. Hu, J.-R. Chen and W.-J. Xiao, *Angew. Chem., Int. Ed.*, 2017, **56**, 1960–1962; (c) S. Roslin and L. R. Odell, *Eur. J. Org. Chem.*, 2017, **2017**, 1993–2007; (d) Z. Zhang, T. Ju, J.-H. Ye and D.-G. Yu, *Synlett*, 2017, **28**, 741–750; (e) W.-J. Zhou, Y.-H. Zhang, Y.-Y. Gui, L. Sun and D.-G. Yu, *Synthesis*, 2018, **50**, 3359–3378; (f) Y. Chen, L.-Q. Lu, D.-G. Yu, C.-J. Zhu and W.-J. Xiao, *Sci. China: Chem.*, 2019, **62**, 24–57.
- For selected examples of allylic C–H oxidation: (a) M. B. Andrus and Z. Zhou, *J. Am. Chem. Soc.*, 2002, **124**, 8806–8807; (b) D. J. Covell and M. C. White, *Angew. Chem., Int. Ed.*, 2008, **47**, 6448–6451.
- For reviews on allylic C–H amination: (a) M. Johannsen and K. A. Jørgensen, *Chem. Rev.*, 1998, **98**, 1689–1708; (b) R. L. Grange, E. A. Clizbe and P. A. Evans, *Synthesis*, 2016, **48**, 2911–2968.
- N. Ishida, Y. Masuda, S. Uemoto and M. Murakami, *Chem.–Eur. J.*, 2016, **22**, 6524–6527.
- (a) B. M. Trost and D. L. Van Vranken, *Chem. Rev.*, 1996, **96**, 395–422; (b) Z. Li and C.-J. Li, *J. Am. Chem. Soc.*, 2006, **128**, 56–57; (c) J. M. Howell, W. Liu, A. J. Young and M. C. White, *J. Am. Chem. Soc.*, 2014, **136**, 5750–5754; (d) R. Zhou, H. Liu, H. Tao, X. Yu and J. Wu, *Chem. Sci.*, 2017, **8**, 4654–4659.
- (a) T. Hoshikawa and M. Inoue, *Chem. Sci.*, 2013, **4**, 3118–3123; (b) M. Sekine, L. Ilies and E. Nakamura, *Org. Lett.*,



2013, **15**, 714–717; (c) J. D. Cuthbertson and D. W. C. MacMillan, *Nature*, 2015, **519**, 74–77; (d) L. Huang and M. Rueping, *Angew. Chem., Int. Ed.*, 2018, **57**, 10333–10337.

8 (a) H. Ding and G. K. Friestad, *Synthesis*, 2005, **2005**, 2815–2829; (b) M. Yus, J. C. González-Gómez and F. Foubelo, *Chem. Rev.*, 2011, **111**, 7774–7854; (c) R. Wang, Y. Luan and M. Ye, *Chin. J. Chem.*, 2019, **37**, 720–743.

9 (a) Y. Yamamoto and N. Asao, *Chem. Rev.*, 1993, **93**, 2207–2293; (b) R. Bloch, *Chem. Rev.*, 1998, **98**, 1407–1438.

10 For a recent review on photoredox catalyzed functionalization of imines, see: (a) J. A. Leitch, T. Rossolini, T. Rogova, J. A. P. Maitland and D. J. Dixon, *ACS Catal.*, 2020, **10**, 2009–2025. For selected examples, see: (b) T. Ju, Q. Fu, J.-H. Ye, Z. Zhang, L.-L. Liao, S.-S. Yan, X.-Y. Tian, S.-P. Luo, J. Li and D.-G. Yu, *Angew. Chem., Int. Ed.*, 2018, **57**, 13897–13901; (c) N. R. Patel, C. B. Kelly, A. P. Siegenfeld and G. A. Molander, *ACS Catal.*, 2017, **7**, 1766–1770; (d) W.-J. Zhou, G.-M. Cao, G. Shen, X.-Y. Zhu, Y.-Y. Gui, J.-H. Ye, L. Sun, L.-L. Liao, J. Li and D.-G. Yu, *Angew. Chem., Int. Ed.*, 2017, **56**, 15683–15687; (e) L. Qi and Y. Chen, *Angew. Chem., Int. Ed.*, 2016, **55**, 13312–13315; (f) E. Fava, A. Millet, M. Nakajima, S. Loescher and M. Rueping, *Angew. Chem., Int. Ed.*, 2016, **55**, 6776–6779; (g) M. Nakajima, E. Fava, S. Loescher, Z. Jiang and M. Rueping, *Angew. Chem., Int. Ed.*, 2015, **54**, 8828–8832; (h) D. Uraguchi, N. Kinoshita, T. Kizu and T. Ooi, *J. Am. Chem. Soc.*, 2015, **137**, 13768–13771; (i) J. L. Jeffrey, F. R. Petronijević and D. W. C. MacMillan, *J. Am. Chem. Soc.*, 2015, **137**, 8404–8407; (j) D. Hager and D. W. C. MacMillan, *J. Am. Chem. Soc.*, 2014, **136**, 16986–16989; (k) For a general review on photocatalytic C–Heteroatom bond formation, see: A. Ruffoni, and D. Leonori, *Photocatalytic Carbon–Heteroatom Bond Formation, Science of Synthesis*, 2019, p. 517.

11 M. Hopfner, D. M. Wei, F. W. Heinemann and H. Kisch, *Photochem. Photobiol. Sci.*, 2002, **1**, 696–703.

12 For recent examples on synergistic organo- and photoredox catalysis, see: (a) A. G. Capacci, J. T. Malinowski, N. J. McAlpine, J. Kuhne and D. W. C. MacMillan, *Nat. Chem.*, 2017, **9**, 1073; (b) A. J. Musacchio, B. C. Lainhart, X. Zhang, S. G. Naguib, T. C. Sherwood and R. R. Knowles, *Science*, 2017, **355**, 727–730; (c) R. Zhou, Y. Y. Goh, H. Liu, H. Tao, L. Li and J. Wu, *Angew. Chem., Int. Ed.*, 2017, **56**, 16621–16625; (d) T. Miura, Y. Funakoshi, J. Nakahashi, D. Moriyama and M. Murakami, *Angew. Chem., Int. Ed.*, 2018, **57**, 15455–15459; (e) W. Xu, J. Ma, X.-A. Yuan, J. Dai, J. Xie and C. Zhu, *Angew. Chem., Int. Ed.*, 2018, **57**, 10357–10361; (f) N. Zhou, X.-A. Yuan, Y. Zhao, J. Xie and C. Zhu, *Angew. Chem., Int. Ed.*, 2018, **57**, 3990–3994; (g) M. Das, M. D. Vu, Q. Zhang and X.-W. Liu, *Chem. Sci.*, 2019, **10**, 1687–1691; (h) Q.-Y. Meng, T. E. Schirmer, A. L. Berger, K. Donabauer and B. König, *J. Am. Chem. Soc.*, 2019, **141**, 11393–11397; (i) M. Zhang, X.-A. Yuan, C. Zhu and J. Xie, *Angew. Chem., Int. Ed.*, 2019, **58**, 312–316; (j) H. Jiang and A. Studer, *Chem. - Eur. J.*, 2019, **25**, 7105–7109.

13 For selected reviews on PCET, see: (a) R. Knowles and H. Layla, *Synlett*, 2014, **25**, 2819–2826; (b) E. C. Gentry and R. R. Knowles, *Acc. Chem. Res.*, 2016, **49**, 1546–1556; (c) D. C. Miller, K. T. Tarantino and R. R. Knowles, *Top. Curr. Chem.*, 2016, **374**, 30; (d) N. Hoffmann, *Eur. J. Org. Chem.*, 2017, **2017**, 1982–1992.

14 K. A. Ogawa and A. J. Boydston, *Org. Lett.*, 2014, **16**, 1928–1931.

15 For reviews on thiyl radicals, see: (a) F. Dénès, C. H. Schiesser and P. Renaud, *Chem. Soc. Rev.*, 2013, **42**, 7900–7942; (b) F. Dénès, M. Pichowicz, G. Povie and P. Renaud, *Chem. Rev.*, 2014, **114**, 2587–2693.

16 Y.-R. Luo, *Handbook of Bond Dissociation Energies in Organic Compounds*, CRC Press, Boca Raton, FL, 2003.

17 For reviews on persistence radical effect, see: (a) A. Studer, *Chem. - Eur. J.*, 2001, **7**, 1159–1164; (b) H. Fischer, *Chem. Rev.*, 2001, **101**, 3581–3610; (c) D. Leifert and A. Studer, *Angew. Chem., Int. Ed.*, 2020, **59**, 74–108.

18 J. Xie, H. Jin and A. S. K. Hashmi, *Chem. Soc. Rev.*, 2017, **46**, 5193–5203.

19 (a) J. L. Schwarz, F. Schäfers, A. Tlahuext-Aca, L. Lückemeier and F. Glorius, *J. Am. Chem. Soc.*, 2018, **140**, 12705–12709; (b) H. Mitsunuma, S. Tanabe, H. Fuse, K. Ohkubo and M. Kanai, *Chem. Sci.*, 2019, **10**, 3459–3465.

20 J. D. Slinker, A. A. Gorodetsky, M. S. Lowry, J. Wang, S. Parker, R. Rohl, S. Bernhard and G. G. Malliaras, *J. Am. Chem. Soc.*, 2004, **126**, 2763–2767.

21 A. Juris, V. Balzani, P. Belser and A. von Zelewsky, *Helv. Chim. Acta*, 1981, **64**, 2175–2182.

22 A. Joshi-Pangu, F. Lévesque, H. G. Roth, S. F. Oliver, L.-C. Campeau, D. Nicewicz and D. A. DiRocco, *J. Org. Chem.*, 2016, **81**, 7244–7249.

23 At the current stage, we can not rule out that the *N*-centered radical abstracts hydrogen atom from benzylic C–H bond to form a benzyl carbon radical, which can be further reduced to generate carbon anion then undergoes protonation to afford the product.

